Science Advances
AAAS

advances.sciencemag.org/cgi/content/full/6/21/eaaz8344/DC1

# Supplementary Materials for

## Interfacing gene circuits with microelectronics through engineered population dynamics

M. Omar Din, Aida Martin, Ivan Razinkov, Nicholas Csicsery, Jeff Hasty*

*Corresponding author. Email: hasty@ucsd.edu

Published 22 May 2020, *Sci. Adv.* **6**, eaaz8344 (2020)
DOI: 10.1126/sciadv.aaz8344

**The PDF file includes:**



**Other Supplementary Material for this manuscript includes the following:**

(available at advances.sciencemag.org/cgi/content/full/6/21/eaaz8344/DC1)

**Supplementary Text**

Impedance basis

A sinusoidal AC potential is applied to the system. The calculated impedance results from the ratio of the applied voltage and the measured current that flows through the system. The impedance spectra are obtained by sequential measurements for each single frequency.

The impedance in aqueous solution is represented by an equivalent circuit. This consists of two components, a double layer capacitor ($C_{dl}$) and bulk medium resistor ($R_s$) connected in series. $C_{dl}$ accounts for the effect of ionic species on the capacitance near the surface of an electrode. $R_s$ represents the bulk resistance of the solution, accounting for the change in conductivity and charge transport across the bulk solution.

There are three regions in the impedance spectrum (see **Figure S1b**). These are represented by two components in the equivalent circuit individually, and their combination. The double layer region dominated by $C_{dl}$ is in the frequency range of 1 Hz to 5 Hz (shaded in green). Resistive region dominated by $R_s$ is in the frequency range between 35 kHz to 100 kHz (shaded in blue). The region dominated by both $C_{dl}$ and $R_s$ is in the frequency range of 5 Hz–35 kHz (not shaded).

The effect of the double layer capacitance is noticeable at phase angle values close to −90º as shown. In the high frequency range, resistive region, the phase angle values are closed to 0º and the magnitude of the impedance is constant, as resistive impedance is independent of frequency.

At the high frequency interval (> 35 kHz) there is no substantial contribution to the double layer capacitance. Thus, the most important contribution to the total impedance of the system at high frequencies is related to the resistance of the medium, which is independent from the frequency. This region is defined as the resistive region, in which ion conduction in the medium is dominant (**Figure S1b**, $R_s$ region). Therefore, the changes in the double layer of the electrode, and the changes in the medium during bacterial growth can be detected by measuring impedance at different frequencies, which is the reason for the present study to explore the microbiological detection at these frequencies.

Impedance characterization

Bacterial cultures and media were studied using 50 µL of sample solution (Fig. S1). The different solutions characterized include fresh LB media ((BD Difco, LB broth, Miller) containing 0.075 % Tween-20), concentrated bacteria mixed with fresh LB media, supernatant from a MG1655 *E. coli* culture grown to an optical density at 600 nm (OD600) of 0.61, and a heat-killed MG1655 culture (10 minutes at 90 °C), at an OD600 of 0.18.

Redox inactivity of the bacteria and LB on the screen printed gold electrodes was characterized using cyclic voltammetry (CV) between -0.5 to +1.0 V with 10 mV potential step at a scan rate of 50 mV/s. CV only showed the oxidation of water to oxygen at high potentials and the reduction to hydrogen at low potentials (Fig. S1a).

Lysis circuits

The synchronized lysis circuit (SLC) constructs consisted in two plasmids an activator (KAN, ColE1), and a lysis plasmid built by taking the lysis gene, E, from the ePop plasmid via PCR and

cloning it into a vector (CM, p15A) under the control of the luxI promoter. The hlyE gene was obtained via PCR from the genomic DNA of MG1655. The SLC strains were cultured in LB media with 50 μg $mL^{-1}$ and 34 μg $mL^{-1}$ of kanamycin (KAN) and chloramphenicol (CM) respectively, along with 0.2 % glucose, in a 37 °C incubator. The stimuli-dependent strains were cultured in LB media with 50 μg $mL^{-1}$ KAN along with 0.2 % glucose, in a 37 °C incubator.

Turbidity sensor

Customized turbidity printed circuit board includes an OPT101 monolithic photodiode with on-chip transimpedance amplifier BPW34 infrared/visible silicon detector and a 950 nm infrared LED emitter (RadioShack, Forth Worth, TX, US). A 555 timer along with a modulator/demodulator (AD630) enable filtered signal. Turbidity values were transmitted via USB to a PC in which sampling time and gain were controlled. Detection was performed at 90° versus the LED every 30 s. (Fig. S3b). Calibration of the turbidity sensor was performed for a growth curve of a MG1655 *E. coli* culture in LB media simultaneously measuring with our customized turbidity board and a spectrometer at 600 nm every 15 min (Fig. S3c).

Milli-fluidic device

Our milli-fluidic devices were constructed from polydimethylsiloxane (PDMS) (Dow Corning, Sylgard 184) which was molded and baked on a silicon master with customized features. The Si wafer formed by cross-linked photoresist consisted in three layers of 4, 30 and 100 μm height, respectively. Individual devices consist of 10 x 9 array bacterial traps of 0.6 mm diameter and 30 μm height connected via two 4 μm height channels to a main channel, which provides fresh media to the individual bacterial cultures. Devices cut out of the baked PDMS and holes are punched in the devices to allow the connection of fluid lines. When electrodes were used for analysis, a conventional mask aligner was required for successful alignment. The devices were then kept for 2 h in a 37 °C incubator for complete bonding. The devices were then placed on a microscope 3D printed stage for imaging and connected to the impedance module. Fluid lines were connected to the device from two syringes one supplying media, and another acting as waste reservoir. Hydrostatic pressure driven flow is controlled by maintaining a 15-inch relative height difference between the inlet and outlet syringes. In these microfluidic experiments we added 0.075 % Tween-20 to the media and cell suspension fluid to prevent cells from adhering to PDMS channels, electrodes, tubing or ports of our device.

Bacterial seeding

For the electrochemostat experiments, 60 μL of overnight culture at an OD600 of 0.6 were added to 3 mL of LB supplemented with 0.075 % Tween-20 and the appropriate antibiotics. The surfactant addition prevented bacteria from adhering to glass, electrodes and tubing.

Bacterial loading on the bIC device was performed by an automatic echo acoustic liquid handler (Labcyte Inc., San Jose, CA, US). The robotic transducer transferred 2.5 nL of overnight culture at and OD600 of 0.8 to each trap. Cells are transferred 10 minutes after exposing glass and PDMS to oxygen plasma for optimal cell loading.

Microscope

We used the same microscopy system as described in our previous group (*36*). Briefly, we used a Nikon Eclipse TI epifluorescent microscope with phase-contrast based imaging. For the

acquisition of images, we used a CoolSNAP HQ2 CCD camera from Photometrics. The microscope and acquisition was controlled by the Nikon Elements software. A plexiglass incubation chamber connected to a heating unit, which encompassed a wide area around the stage, was used in order to maintain the temperature of the microfluidic device at 37 °C. Phase-contrast images were taken at 10x magnification at 10-50 ms exposure times. Fluorescent imaging at 10x was performed at 200 ms for GFP, 30 % setting on the Lumencor SOLA light source. Images were taken every 4 minutes for the course of a typical experiment.

Data analysis

For the electrochemostat, data from PSTrace software was used including plotting the reciprocal of the total impedance value overtime. Data for turbidity and impedance was smoothed with 5 points of window using a polynomial order 2 and a Savitzky-Golay method, to mitigate temperature fluctuations in the incubator.

For the microfluidic device, microscope images were treated with Image J. The reciprocal of transmitted light intensity profiles were obtained by analyzing frames in Image J from the phase/contrast channel and plotting the mean pixel intensity over time. The reciprocal of that plot is the presented in the Figures. Electrochemical plots were obtained from PSTrace software and admittance was calculated from the total value of impedance.

In Figure 4C, to better visualize the contrast between growing cells and empty space, transmitted light values in the cell traps that fell below a threshold value indicative of cell growth were made red and superimposed with the original video.

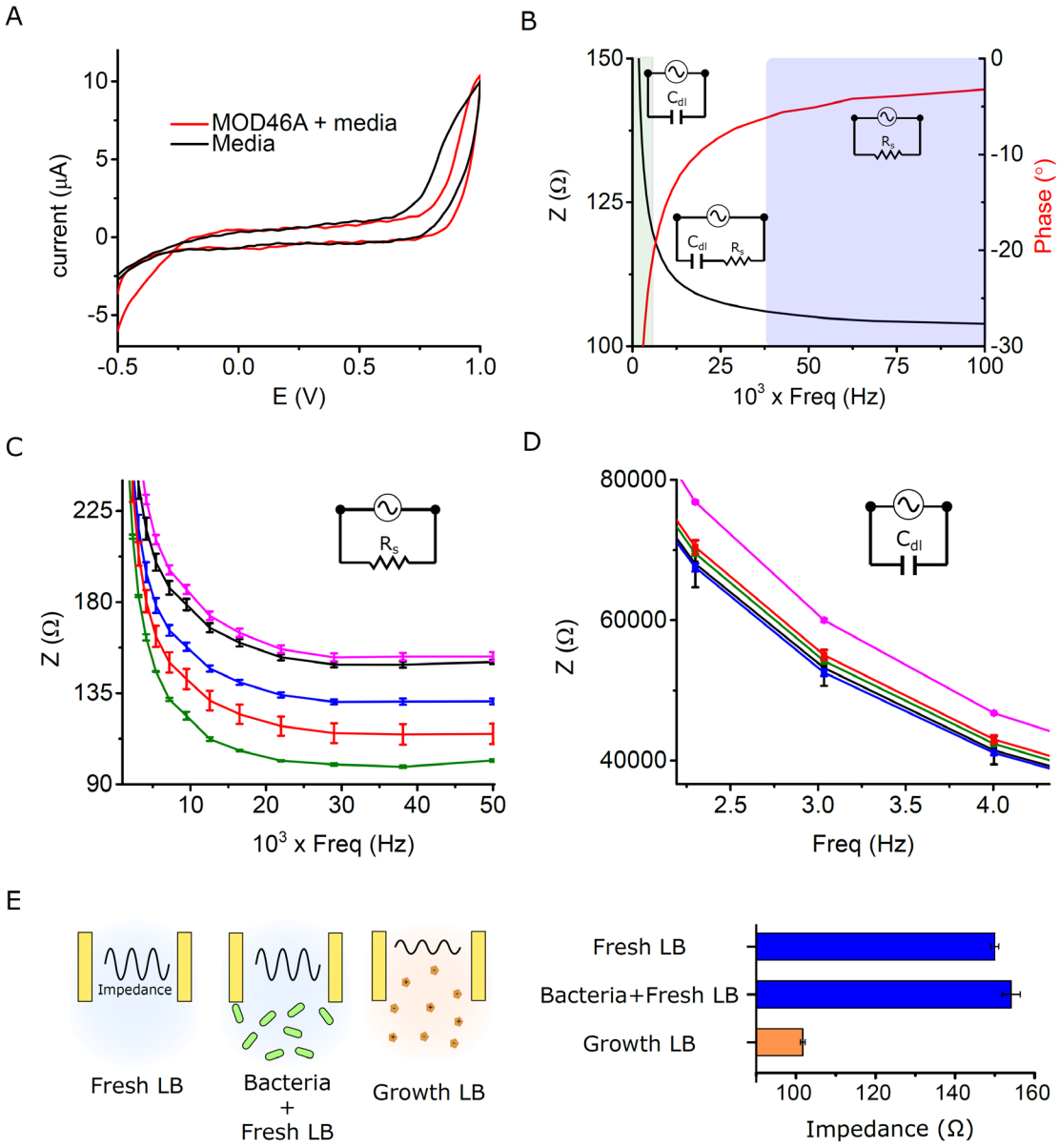


**Fig. S1.**

Electrochemical impedance spectroscopy characterization. (**A**) Cyclic voltammetry showing the inert redox response of MOD46A strain in growing media (red line) and media in absence of cells (black line). (**B**) Impedance versus frequency plot or Bode plot for MOD46A strain including impedance (black line) and phase (red line) and correspondent equivalent circuits in the different range of frequencies. (**C**) Bode plots for fresh LB media (black line), only bacteria (magenta line), supernatant (green line), saturated culture (red line), and heat-killed culture (blue line) between 1000 to 50,000 Hz, where impedance measures resistive effects. Error bars show standard deviation for n=3 samples. (**D**) Bode plots between 1.5 and 4 Hz, where the equivalent circuit corresponds to a capacitor as in (c). (**E**) Schematic and histogram showing the different impedance contributions without additional redox mediators from fresh LB media, a solution of fresh LB with

concentrated bacteria, and depleted LB medium resulting from bacterial growth. Error bars represent standard deviation for n=3 samples.

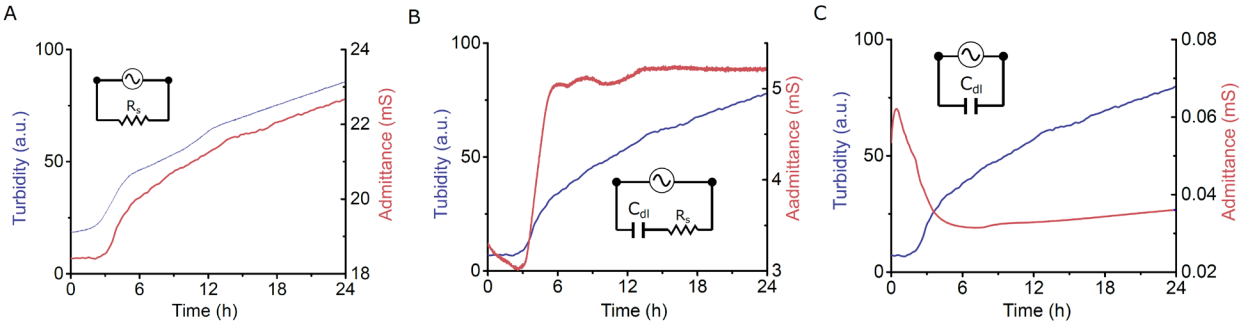


**Fig. S2.**

Signal optimization using wild-type bacteria. (**A**) Profiles of turbidity (blue) and admittance (red) for MG1655 *E. coli* at 100 kHz, (**B**) intermediate 1.5 kHz frequencies, and (**C**) low 1 Hz frequencies, and correspondent equivalent circuits.

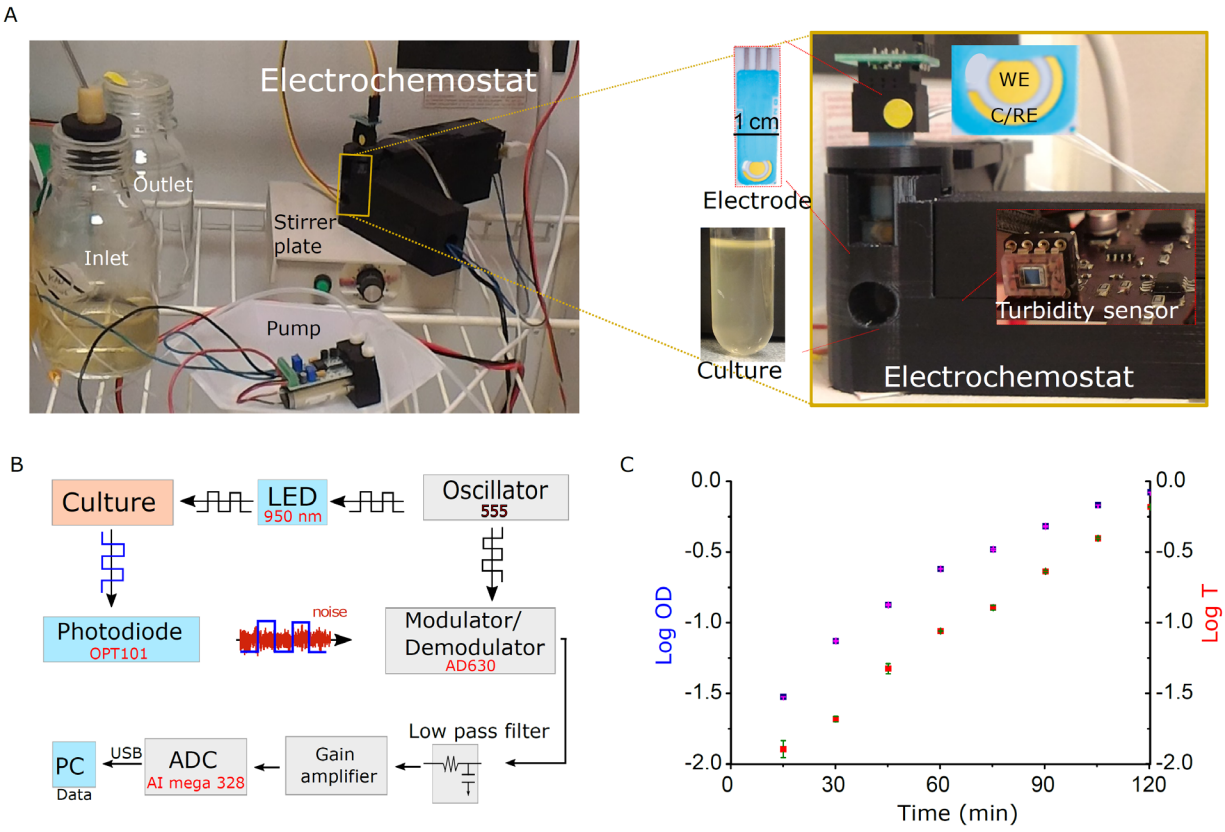


**Fig. S3.**

Electrochemostat set-up and performance. (**A**) Picture of `electrochemostat' components included in a 3D printed holder containing a culture tube, in which the disposable electrode consisting of gold counter/reference (C/RE) and working (WE) electrodes are immersed, and a printed turbidimeter circuit board. (**B**) Complete macro-chemostat set-up showing the pumping system under continuous mixing conditions. (**C**) Schematic of customized turbidity sensor working principle. d, Correlation between Log Turbidity (red) sensor and Log Optical density (blue) at 600 nm using a culture containing MG1655 *E. coli*. Error bars show standard deviation for n=3 samples. Photo credit: M. O. Din, UCSD.

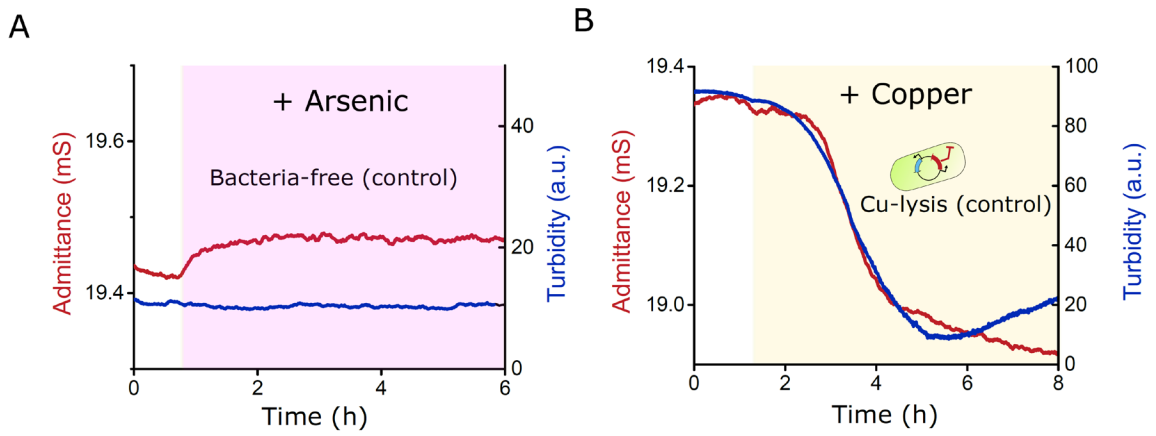


**Fig. S4.**

Controls for the bacterial approach. (**A**) Admittance (red) and turbidity (blue) profiles for LB media in absence of bacteria with shaded region representing induction with 250 ppb arsenic. (**B**) Profiles for copper detection using copper-sensitive strain with shaded region representing induction with 250 ppb copper.

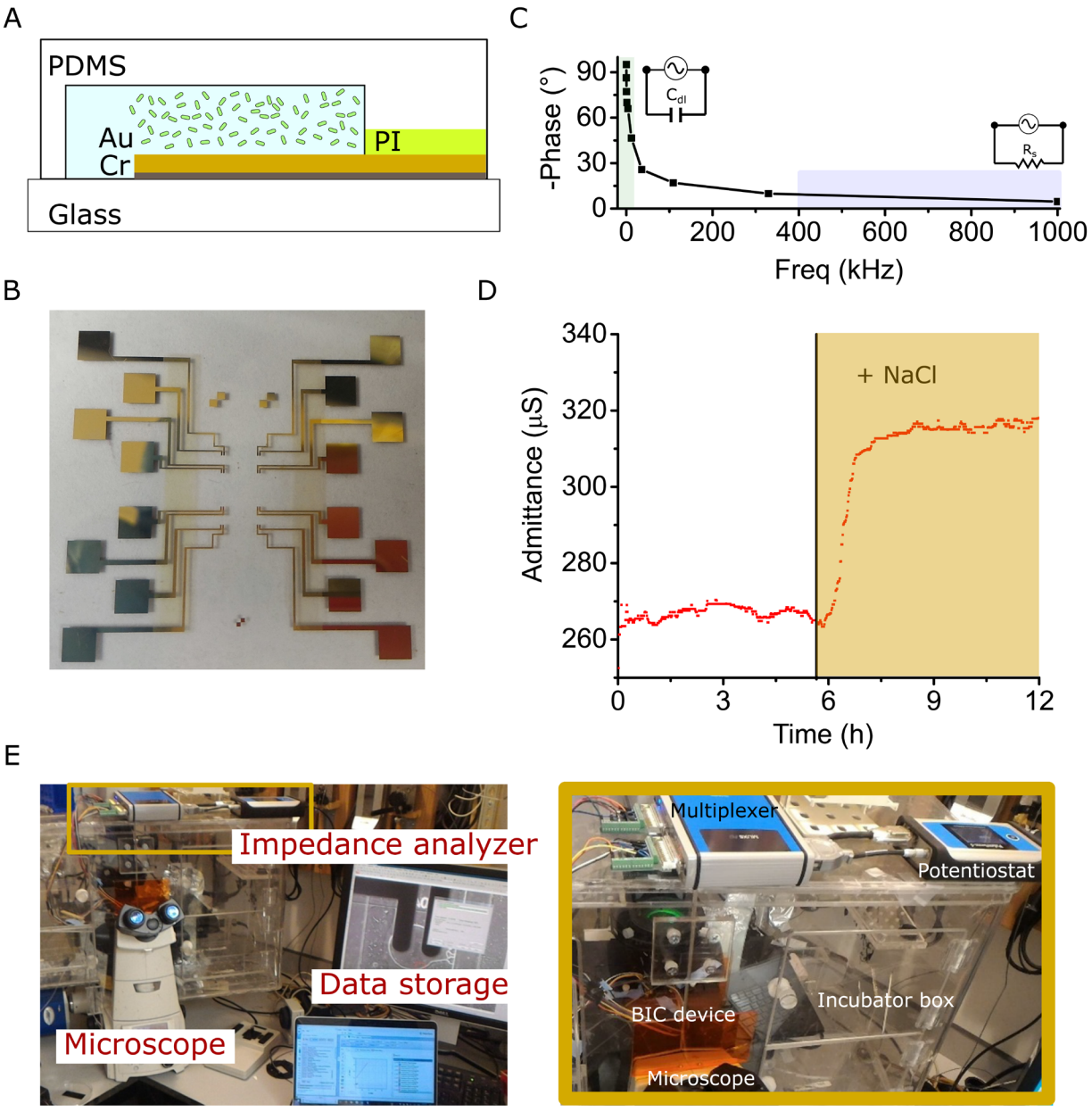


**Fig. S5.**

bIC set-up and performance. (**A**) Schematic of fabrication of electrode's in bIC on glass consisting in a sequential deposition of conductive chrome and gold layers and a final spin of a polyimide insulator layer. (**B**) Picture of the lithography fabricated electrodes on glass. (**C**) Bode plot in bIC for LB media and correspondent equivalent circuits at different frequencies. (**D**) Admittance response of microfluidic electrodes using LB, induced with 100 µM NaCl (shadowed yellow) using same procedure than with multiple bICs. (**E**) Picture of the complete set-up used for bIC data acquisition including microscope and impedance analyzer. Photo credit: M. O. Din, UCSD.

**Movie S1.**

Timelapse microscopy showing transmitted light of the synchronized lysis circuit (SLC) at 4X magnification in a bIC device. Bacterial growth chambers on the top and bottom are connected to gold electrodes and images were taken every 10 min.

**Movie S2.**

Timelapse microscopy showing transmitted light of the arsenic-lysis strain at 10X magnification in one bIC chamber. The bacterial growth chamber is connected to gold electrodes and images were taken every 4 min.